JMEPEG (2007) 16:752–756
DOI: 10.1007/s11665-007-9086-3

1059-9495/$19.00

Influence of Indium Trace Addition on the Precipitation Behavior in a 357 Cast Aluminum Alloy

Guiqing Wang, Qingzhou Sun, Li Shan, Zhongkui Zhao, and Liu Yan

(Submitted May 22, 2006; in revised form September 26, 2006)

Effect of indium addition on aging precipitation behavior of 357 cast alloy has been investigated by hardness measurement, differential scanning calorimetry (DSC) and TEM analysis. Age hardening results show that 0.1 wt.% indium addition to 357 cast alloy increases the peak hardness by 20 HV during aging at 160 °C. DSC and TEM analysis results show that indium addition constrains precipitation of GP zones, and enhances precipitation of β″ phases. The possible indium atoms participating in the precipitation during aging and the large indium-vacancy binding energy can explain the effect of indium on aging behavior of 357 cast alloy.

Keywords aging behavior, aluminum alloy, precipitates, effect of indium

1. Introduction

Cast Al-Si-base alloys are used extensively in many applications requiring a high strength-to-weight ratio because of an excellent combination of castability and mechanical properties, as well as good corrosion resistance and weldability. Many castings are normally heat treated to the T6 condition in order to obtain higher strength and hardness through the formation of a large number of nm-size precipitates that strengthen the soft aluminium matrix (Ref 1-3). The strength and hardness in the casting after T6 treatment are significantly influenced by various process parameters such as solution treatment temperature and time, quenching conditions, natural aging, and artificial aging conditions (Ref 4-6). In addition, minor alloying is an effective method to improve the age hardening in age hardenable aluminum alloys (Ref 7-9). Investigations have shown that any delay between quenching and artificial aging (room temperature storage, termed natural aging or delayed aging) leads to severe deterioration in age hardening response and certain trace additions such as cadmium, indium, and tin can counteract the harmful effects of natural aging on age hardening response (Ref 1, 7, 10, 11). Murali et al. (Ref 7) explained that for Al-7Si-0.3Mg alloy having trace element cadmium, cadmium would act as an active trace element to trap magnesium atoms to reduce the lattice strain energy and, hence, as a result reduce the rate of aging at room temperature. The impurity-vacancy interaction theory was also used to explain this experimental observation (Ref 11). It should read the mechanism by which trace elements In and Sn affect the nucleation and growth of precipitates in an Al-Ag alloy is to reduce the number of quenched-in dislocation loops because of the high-solute/vacancy binding energy of In and Sn (Ref 12). However, no detailed study of such trace addition on age precipitation behavior of Al-Si-base alloys has been carried out and the results that are available are scarce. The present study was carried out to investigate the effect of adding 0.1% indium to 357 cast alloy on age precipitation behaviors by DSC and TEM analysis. Hardness measurement was used to examine the age hardening progress.

Guiqing Wang, Qingzhou Sun, Zhongkui Zhao, and **Liu Yan,** Department of Material Science and Technology, Shandong Architectural University, Ji'nan 250101, P.R. China; **Li Shan,** Jinan Science and Technology Information Research Institute, Ji'nan 250062, P.R. China. Contact e-mail: wangguiqing@126.com.

2. Experiments

High-purity Al, Mg, Si, and indium were used in the preparation of 357 (Al7Si0.4 Mg,wt.%) and 0.1 wt.% indium containing 357 alloys. The alloys were prepared in an electric resistance furnace. The melt was held at 710 °C for about 10 min to ensure complete homogenization, and then poured into a permanent mould. All cast samples used in this work are 16 mm in diameter from permanent mould.

An electric furnace with a temperature control of ±3 °C was used for heat treatment. Casting samples were solution treated at 530 ± 3 °C for 10 h followed by quenching in 25 °C water immediately, natural aged for 24 h and then artificially aged at 160 ± 3 °C for 2-15 h. Hardness testing was carried out using macro Vickers hardness tester with a load of 19.8 N and a dwell time of 30 s. Each Vickers hardness value was the average of at least five measurements.

DSC analysis was performed using a differential scanning calorimeter (NETZSCH DSC 404). Nonmetallic crucibles (Al_2O_3) were used. DSC samples of 20-30 g were punched from bars for DSC analysis. The isothermal DSC runs were carried out as: placing a sample in the sample pan, the cell equilibrated at 25 °C and then heated to 160 °C at a heating rate of 10 °C/min, holding at this temperature for 15 h, the isothermal DSC test was carried out and relative curve was obtained. The continuous heating DSC runs were carried out as: placing a super purity aluminum sample in the sample pan, the

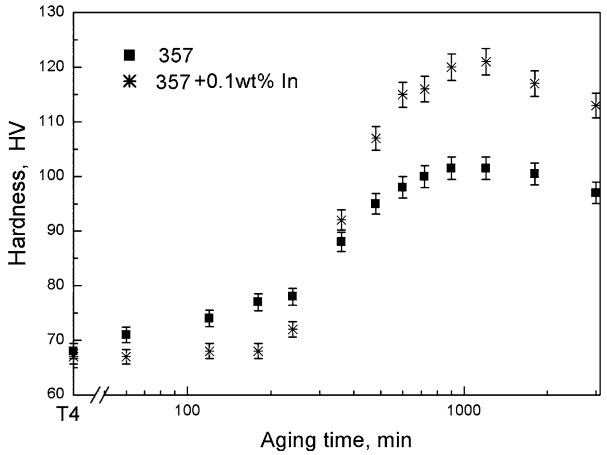

Fig. 1 Hardness vs. age time during aging at 160 °C

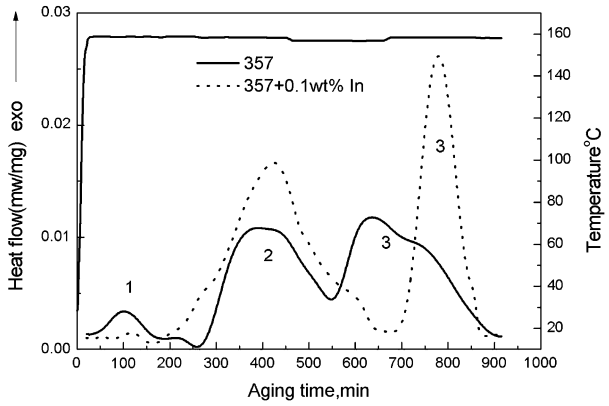

Fig. 2 Isothermal DSC curves at 160 °C

cell equilibrated at 25 °C and then heated to 650 °C at a heating rate of 10 °C/min under an argon atmosphere with a flow rate of 80 mL/min, a super purity Al baseline run was carried out and relative baseline run was obtained. After this operation, placing a sample of equal mass in the same pan, repeating the upper operation, the sample run was obtained. The heat effects associated with the transformation reactions were obtained by subtracting the super purity Al baseline.

TEM samples were cut to 0.5 mm thick by an electrical discharge wire—cutting machine. Thin samples were mechanically polished to 0.1 mm and then thin foils transparent for electronic beam were obtained using an ion polish machine. Microstructures were observed using a H-800 TEM operated at 150 kV.

3. Results and Analysis

3.1 Age Hardening Analysis

Figure 1 shows age hardening curves for 357 and 0.1 wt.% indium containing 357 alloy aged at 160 °C. For the 357 alloys, hardness increases during aging 60 min and peak hardness value 103 HV is obtained during aging about 900 min. For indium containing alloy, there is only a slight hardness increasing during aging about 180 min, but hardness increases quickly during aging 200-700 min and peak hardness value 123 HV is obtained during aging about 900 min. This suggests that 0.1% indium addition to the 357 alloy increases the age hardening response significantly.

3.2 Age Precipitation Analysis

A DSC run yields the heat flow (heat release or absorption), dH/dt, due to the phase transformation as a function of time under a constant temperature. The area under a DSC peak reflects the heat effects (enthalpy) associated with this transformation and is proportional to the volume fraction of phases precipitating (or dissolving) during this stage.

DSC curves during aging at 160 °C are shown in Fig. 2. Three exothermal peaks 1, 2, 3 appear in DSC curves for both alloys. Assuming the generally accepted sequential representations during age precipitation in Al-Si-Mg alloys, exothermal peaks 1, 2, 3 should be associated with the precipitation of GP zones, coherent β″ phases, semicoherent β′ phases respectively.

Comparing Fig. 2 with Fig. 1, hardness increases with the precipitation of GP zones and quick age hardening corresponds with the precipitation of coherent β″ phases. Although the volume fraction of precipitates increasing with the transformation of β″ to β′, the age hardening rate decreases and peak hardness is obtained before β′ transforming to β phases. Hardness will decrease with the coarsing and transformation of β′ phases to β phase.

Figure 2 shows that the heat effects associated with the precipitation of GP zones (the area of peak 1) for indium containing 357 alloy is smaller than that of 357 alloy, but heat effects associated with the precipitation of β″ phases (the area of peak 2) for indium containing 357 alloy is obviously bigger than that of 357 alloy. This suggests that 0.1 wt.% indium addition to 357 alloy constrains the precipitation of GP zones, but enhances the precipitation of β″ phases. Combining with age hardening analysis results, it suggests that indium addition decreases the age hardening rate by constraining the precipitation of GP zones at early stage of aging, and increases the age hardening response by enhances the precipitation of β″ phases.

3.3 TEM Analysis

Figure 3 shows TEM micrographs both of 357 and indium containing 357 alloys aged at 160 °C for 120 min, respectively. The contrast effect reflects the crystal distortion due to the precipitation of GP zones coherent with α(Al). Comparing Fig. 3(b) with Fig. 3(a), less GP zones appeared for indium containing 357 alloy, instead of it, many dislocation loops formed.

Figure 4(a, b) are TEM micrographs for 357 and indium containing 357 alloys aged at 160 °C for 900 min respectively. Both coherent β″ phases and semicoherent β′ phases are detected by analyzing the selected area diffraction patterns for two alloys. It is shown that smaller fine precipitates are coherent β″ phases and needle shaped precipitates are semicoherent β′ phases. Comparing Fig. 4(b) with Fig. 3(b), it can be seen that the dislocation loops shown in Fig. 3(b) have been replaced by finely distributed β″ phases as shown in Fig. 4(b). Comparing Fig. 4(a) with Fig. 4(b), the β″ precipitates density for indium containing alloy is higher than that of the base alloy, which is consistent with the above DSC analysis results that

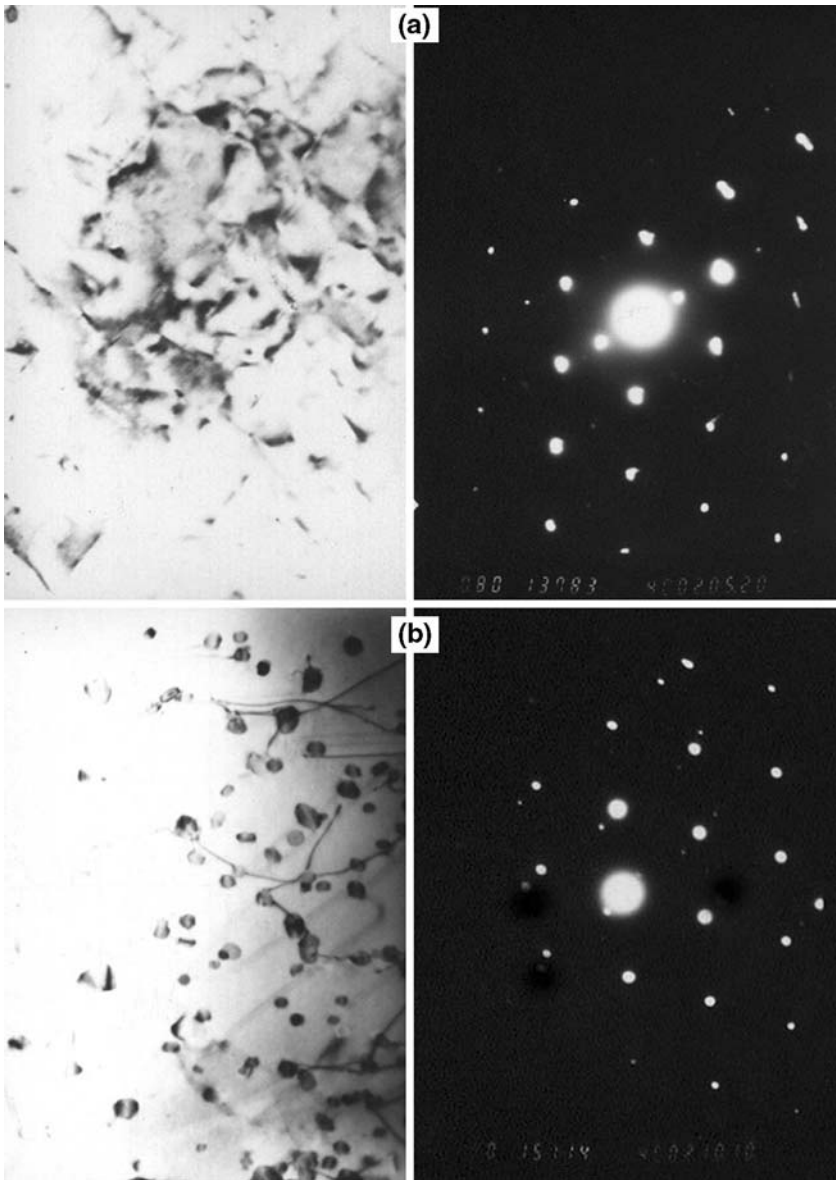

Fig. 3 (a)—357 alloy; (b)—0.1 wt.% indium containing 357 alloy

indium addition constrains the precipitation of GP zones and increases the volume fraction of β'' precipitates.

4. Discussions

From the experiment results, the benefit effects of indium addition on aging response of 357 alloy is attributed to the effect of indium on precipitation behavior.

Figure 5 shows DSC curves for as-cast samples of both alloys at high-temperature stage. It reflects the effect of indium on precipitation of polynary eutectic phases. It should read that peaks 1 and 2 in DSC curve of 357 alloy should correspond to the following reactions (Ref 13).

Reaction of peak 1: $\alpha(\mathrm{Al}) + \mathrm{Si}(+\mathrm{Al_5SiFe} + \cdots) \rightarrow \mathrm{Liq.}$
Reaction of peak 2: $\alpha(\mathrm{Al}) + \mathrm{Mg_2Si} + \mathrm{Si} \rightarrow \mathrm{Liq.}$

It is obvious that peak 2 shifts to lower temperature in indium containing alloy. This suggests that indium atoms are involved in the precipitation of eutectic phases $\alpha(\mathrm{Al}) + \mathrm{Mg_2Si} + \mathrm{Si}$ and make its melting point to low temperature. During solution treatment and quenching, eutectic phases dissolve and α(Al) is supersaturated with Mg, Si, and indium atoms. While the quenched sample is heated to aging temperature, indium atoms are involved in the formation of precipitates (precursors of $\beta(\mathrm{Mg_2Si})$ during aging.

After solution treatment and quenching, dislocations should be introduced into α(Al) to release thermal stresses that are generated during quenching because of the difference of thermal expansion coefficient between α(Al) and eutectic Si, which are the ideal trap of supersaturated vacancies. For 357 alloy, most supersaturated vacancies sink in these dislocations and the concentration of supersaturated vacancies in α(Al) decreases during natural aging or heating to artificial aging

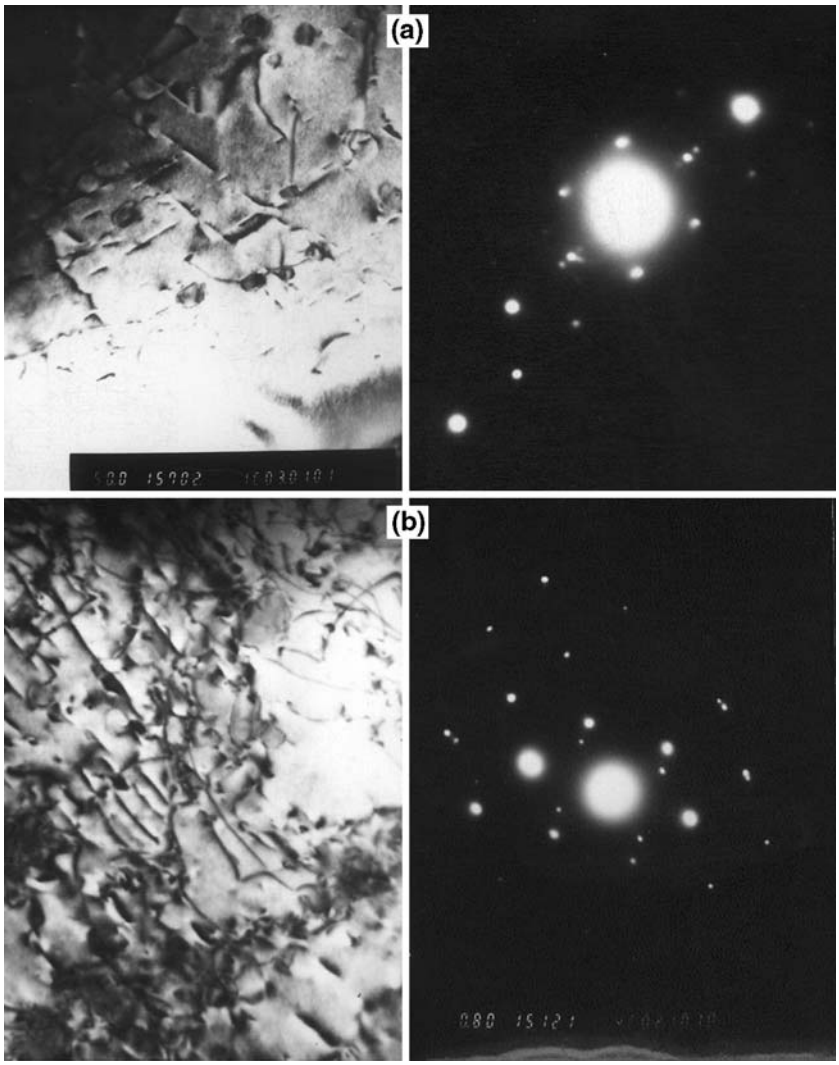

Fig. 4 (a)—357 alloy; (b)—0.1 wt.% indium containing 357 alloy

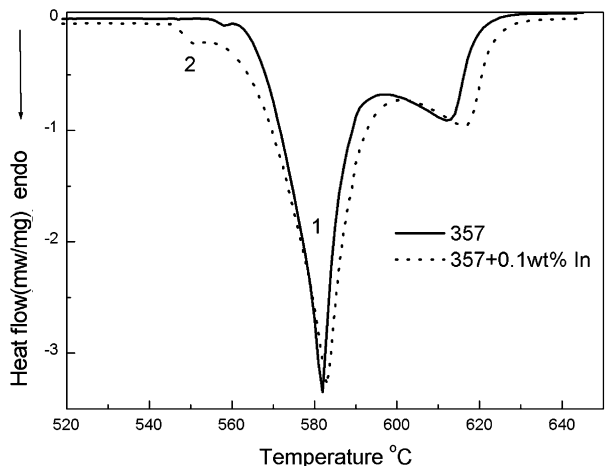

Fig. 5 DSC curves for as-cast samples at a heating rate of 10 °C/min

temperature, which lead to the lower density of GP zones and β″ phases precipitating during aging.

The above microstructure and DSC analysis show that the precipitation of GP zones is constrained, but the precipitation of β″ phases is enhanced while adding 0.1 wt.% indium to 357 alloy. This can be explained by the indium atoms participating in the precipitation and the higher indium-vacancy binding energy in aluminum alloy (0.39 eV (Ref 11)). For indium containing alloy, quenched-in vacancies are bounded by indium, which inhibited the diffusivity of Mg and Si atoms to form GP zones during natural aging or the heating period. As aging progresses, the vacancies, initially bound by indium, are released and condense forming dislocation loops surrounded by indium atoms, which easy act as the heterogeneous nucleation of β″ phases because of the low-surface energy of indium.

The vacancy release mechanism described here has been mentioned in reference (Ref 14), which investigated the effect of Li on the aging behaviors of Al-Cu-Mg alloy by Gregson et al. They reported that there are low-concentration vacancies by the presence of Li atoms owing to high-Li-vacancy binding energy. On aging, during which δ′ precipitates (formed during quenching), a large number of vacancies are released and condense forming dislocation loops, which act as nucleation sites for δ′ phase precipitation, with the Li atoms being consumed in the formation of δ′. The results of the present investigation suggest

that the indium atoms released from vacancies during the transformation enter into the β″ phase itself.

5. Conclusions

Indium addition to 357 alloy increases the age hardening response during artificial aging.

Indium addition to this alloy delays the precipitation of GP zones but increases the volume fraction of β″ precipitates.

The indium atoms participating in the precipitation during aging and big indium-vacancy binding energy may explain the effect of indium on aging behavior of 357 alloy.

Acknowledgments

We gratefully acknowledge the support of Shandong Science and Research Foundation for Encourageing Exemplary Middle and Young People (Grant No. 2004BS04014).

References

1. S. Shivkumar, C. Keller, and D. Apelian, Aging Behavior in Cast Al-Si-Mg Alloys, *AFS Trans.*, 1990, **98**, p 905–911
2. R.X. Li, R.D. Li, Y.H. Zhao, L.Z. He, C.X. Li, H.R. Guan, and Z.Q. Hu, Age-hardening Behavior of Cast Al-Si Base Alloy, *Mater. Lett.*, 2004, **58**(15), p 2096–2101
3. C.H. Caceres and Q.G. Wang, Solidification Conditions, Heat Treatment and Tensile Ductility of Al-7Si-0.4Mg Casting Alloys, *AFS Trans.*, 1996, **104**, p 1039–1043
4. D.L. Zhang, L.H. Zheng, and D.H. Stjohn, Effect of a Short Solution Treatment Time on Microstructure and Mechanical Properties of Modified Al-7wt.%Si-0.3wt.%Mg Alloy, *J. Light Metals*, 2002, **2**, p 27–36
5. P. Ouellet and F.H. Samuel, Effect of Mg on the Ageing Behavior of Al-Si-Cu 319 Type Aluminum Casting Alloys, *J. Mater. Sci.*, 1999, **34**(19), p 4671–4697
6. M.A. Moustafa, F.H. Samuel, and H.W. Doty, Effect of Mg and Cu Additions on the Microstructural Characteristics and Tensile Properties of Sr-modified Al-Si Eutectics Alloys, *Int. J. Cast Metals Res.*, 2002, **14**, p 235–253
7. S. Murali, K.S. Raman, and K.S.S. Murthy, Effect of Iron Impurity and a Cd Trace Addition on the Delayed Ageing of Al-7Si-0.3Mg Casting Alloy, *Cast Metals*, 1991, **2**(1), p 31–36
8. P. Sepehrband, R. Mahmudi, and F. Khomamizadeh, Effect of Zr Addition on the Aging Behavior of A319 Aluminum Cast Alloy, *Scripta Mater.*, 2005, **52**(4), p 253–257
9. Y.J. Li, S. Brusethaug, and A. Olsen, Influence of Cu on the Mechanical Properties and Precipitation Behavior of AlSi7Mg0.5 Alloy during Aging Treatment, *Scripta Mater.*, 2006, **54**(1), p 99–103
10. W.F. Miao and D.E. Laughlin, A Differential Scanning Calorimetry Study of Aluminum Alloy 6111 with Different Pre-aging Treatments, *J. Mater. Sci. Lett.*, 2000, **19**, p 201–203
11. K.T. Kashyap, S. Murali, and K.S. Raman, Casting and Heat Treatment Variables of Al-7Si-Mg Alloy, *Mater. Sci. Technol.*, 1993, **9**(3), p 189–203
12. N. Prabhu and J.M. Howe, The Effect of Ternary Trace Additions on the Nucleation and Growth of Gamma Prime Precipitates in an Al-4.2 at. pct. Ag Alloy, *Met. Trans. A*, 1992, **23**, p 135–138
13. L.F. Mondolfo, *Aluminum Alloys*: *Structure and Property* (in Chinese), Translated by Wang Zhutang, Zhang Zhenlu, and ZHENG Xuan, Pub. Metallurgical industry Press, Beijing, 1988, p 239−240, 203–204, 586–593
14. P.J. Gregson, H.M. Flower, and C.N.J. Tite, Role of Vacancies on Coprecipitation of δ′- and S-Phases in Al-Li-Cu-Mg Alloys, *Mater. Sci. Technol.*, 1986, **2**(3), p 349–360